Vol 12 No 10, October 2003
1009-1963/2003/12(10)/1087-09
Chinese Physics
© 2003 Chin. Phys. Soc.
and IOP Publishing Ltd

The periodic magnetized cylinder tube for atom guidance: quantized motion analysis*

Li Dai-Jun(李代军), Zhou Bo(周 博),
Hu Zheng-Feng(胡正峰), and Li Shi-Qun(李师群)

Department of Physics, Centre for Atomic and Molecular Nanoscience, Tsinghua University, Beijing 100084, *China*

Key Laboratory of Quantum Information and Measurement, Ministry of Education, Beijing 100084, *China*

(Received 2 December 2002; revised manuscript received 18 May 2003)

We have analysed the transport efficiency of an atomic waveguide constructed from a periodic axially magnetized hollow tube. We took into consideration the quantized motion of the atom inside the magnetic hollow cylinder tube, which is significant for the transportation of cold atoms. We deduced the quantized motion modes of the atomic waves in the tube by the approximation of infinite potential, which is valid for cold atoms and strong magnetization. For the atomic waveguide with weak magnetization, we have calculated the tunnelling effect of the atomic wave. The adiabatic condition for the motion of cold atoms is discussed. A time orbit potential method for solving the "zero magnetic field problem" is proposed.

Keywords: atomic waveguide, periodic axially magnetized hollow tube, time orbit potential
PACC: 3280P, 4250, 0365

1. Introduction

Atom optics is a blossoming field originating from atomic physics and optical physics.[1] In this field, the atom exhibits a wave-like nature which shares similarity with light waves in conventional optics. With the rapid development of atom cooling techniques, the wave aspect of the atom is so prominent that many new features such as atomic diffraction, interference and Bose–Einstein condensation (BEC) are observed.[2−4] As a result, these new properties of atoms enable the construction of a new type of atom optical devices. Atomic waveguide is one of such devices which guide the atom along the direction required from one place to another with trivial loss. In our previous papers,[5−7] we proposed the model for atom waveguide using a periodic-magnetized tube and analysed the transport efficiency by a classical method.

For an ultra-cold atom, its wave nature makes the quantum effects (such as quantum tunnelling and quantum reflection) important and the classical treatment fails to discuss the behaviour of this kind of atoms.

In this paper, we employ the quantum theory to study the properties of quantized motions inside the magnetic tube, including the modes of the atomic wavepacket, the tunnelling effect of the atoms, and the influence of the change of magnetic field directions on the adiabatic motion of the atom in the magnetic field. Time orbit average potential (TOP) technique[8] is firstly used in order to overcome the zero point effect of the magnetic field on the adiabatic motion of the atoms.

2. The model Hamiltonian for the periodic magnetized tube

The periodic magnetized tube model, which we proposed previously, is illustrated in Fig.1. The hollow cylindrical tube, with an inner radius a and a thickness of magnetic coating t, is magnetized with a period λ along the axial direction of the tube. If the magnetization is sinusoidal, that is, $M(z) = M_0 \cos kz$, in which $k = 2\pi/\lambda$ is the wavenumber of magnetization, the magnetic field inside the tube could be obtained in the following form:

$$B_\rho = -B_1 \mathrm{I}_1(k\rho)\sin(kz), \tag{1}$$

$$B_z = -B_1 \mathrm{I}_0(k\rho)\cos(kz), \tag{2}$$

*Project supported by the National Natural Science Foundation of China (Grant No 19975027) and the State Key Development Program for Basic Research of China (Grant No 001CB309308).

where $B_1 = \mu_0 M_0[kaK_1(ka) - k(a+t)K_1(k(a+t))]$, in which μ_0 is the magnetic permeability of free space and K_1 is the second kind of first-order modified Bessel function, and I_ν is the first kind of modified Bessel function of the order of ν.

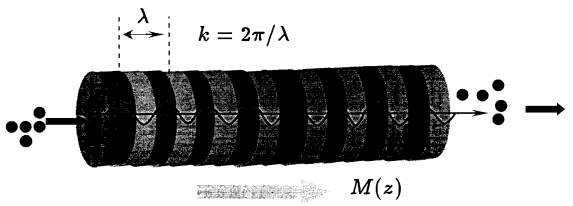


Fig.1. The hollow tube model of atomic waveguide with periodic magnetization. The magnetization is sinusoidal along the tube axis and λ is the period of the magnetization.

The profile of magnetic induction lines in one of the cross sections is illustrated in Fig.2. So the interaction Hamiltonian between the atom and the magnetic field is

$$H_{\rm m} = -\boldsymbol{\mu} \cdot \boldsymbol{B}. \tag{3}$$

Assuming that the total spin of the atom is F, we have the interaction Hamiltonian as follows when the motion of the atom in the magnetic field is adiabatic:

$$H_{\rm m} = \mu_{\rm B} g_F M_F |B|, \tag{4}$$

where $\mu_{\rm B}$ is the Bohr magneton, g_F is Lande factor, and M_F is magnetic quantum number. Under the condition of $ka \gg 1$, Eq.(4) becomes

$$H_{\rm m}(\rho, z) = g_F \mu_{\rm B} M_F \frac{\mu_0 M_0}{2} \times \left[1 - \sqrt{\frac{a+t}{a}} {\rm e}^{-kt}\right] {\rm e}^{-k(a-\rho)}. \tag{5}$$



Fig.2. The profile of magnetic induction lines at a cross section.

Once the atom is trapped inside the magnetic tube, the van der Waals interaction between the wall and atoms will exhibit effects near the wall of the magnetic tube. This interaction is the result of the atomic dipole affected by its electrostatic image in the magnetic coating and can be described by the following equation,

$$H_{\rm vdw} = -\frac{c_{\rm vdw}}{(a-\rho)^3}, \tag{6}$$

where $c_{\rm vdw}$ is expected to be of the order of $1{\rm kHz}\mu{\rm m}^3$.[9] So the Hamiltonian for the motion of the atom in the magnetic tube is

$$\hat{H} = \frac{\hat{P}^2}{2M} + H_{\rm m} + H_{\rm vdw}. \tag{7}$$

Here $\hat{P}$ is the momentum of the atom. We assume that the atomic motion is adiabatic in the magnetic field. Figure 3 illustrates the magnetic interaction potential modified by the van der Waals force between the atom and the wall of the magnetic tube. The depth of the magnetic interaction potential is reduced as the van der Waals interaction is attractive near the wall of the tube in a range of several tens of nanometre. From Eq.(5), one can find that the magnetic field exists just near the wall and reduces exponentially away from the wall. In order to simplify the calculation, we make the following approximation to the potential:

$$V(\rho) = \begin{cases} 0 & (\rho < a - \Delta), \\ V_0 & (a - \Delta \le \rho < a), \\ -V_{\rm m} & (\rho \ge a), \end{cases} \tag{8}$$

where V_0 can be defined by the peak value of the sum of $H_{\rm m}$ and $H_{\rm vdw}$, and $V_{\rm m} \gg V_0$, Δ is the width of the potential. In the following section, we will discuss the motion of the atom in the potential (8).

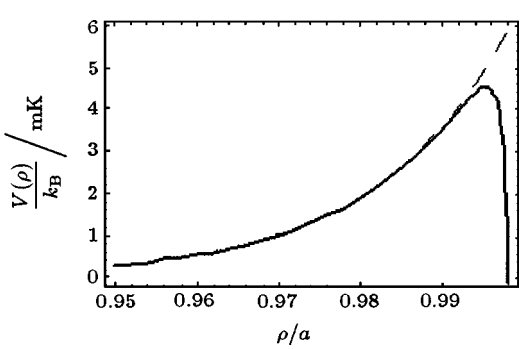


Fig.3. The magnetic interaction potential modified by the van der Waals force between the atom and the wall of the magnetic tube.

3. The adiabatic motion of the atom inside the waveguide

Because the potential described by Eq.(8) has a cylindrical symmetry, it is convenient to describe the

motion of the atom by the Schrödinger equation in cylindrical coordinates and the wavefunction of the atom takes the following form:

$$\Psi(\rho,\phi,z) = R(\rho)\exp(\mathrm{i}m\phi)\exp(\mathrm{i}\beta z), \tag{9}$$

where m is integral due to the natural periodic boundary condition in the azimuthal direction and β is determined by the atomic velocity along z direction. The radial wavefunction satisfies the following equation:

$$\frac{\mathrm{d}^2R}{\mathrm{d}\rho^2} + \frac{1}{\rho}\frac{\mathrm{d}R}{\mathrm{d}\rho} + \left(\frac{2M(E-V(\rho))}{\hbar^2} - \beta^2 - \frac{m^2}{\rho^2}\right)R = 0. \tag{10}$$

Using the following substitutions:

$$\delta_1 = \frac{2Ma^2}{\hbar^2}\left(E - \frac{\hbar^2\beta^2}{2M}\right),$$
$$\delta_2 = \frac{2Ma^2}{\hbar^2}\left(V_0 - E + \frac{\hbar^2\beta^2}{2M}\right),$$
$$\delta_3 = \frac{2Ma^2}{\hbar^2}\left(V_\mathrm{m} + E - \frac{\hbar^2\beta^2}{2M}\right),$$

Eq.(10) takes diverse forms in different regions of the potentials defined by Eq.(8)

$$\frac{\mathrm{d}^2R}{\mathrm{d}\rho^2} + \frac{1}{\rho}\frac{\mathrm{d}R}{\mathrm{d}\rho} + \left(\frac{\delta_1}{a^2} - \frac{m^2}{\rho^2}\right)R = 0 \quad (\rho < a - \Delta),$$
$$\frac{\mathrm{d}^2R}{\mathrm{d}\rho^2} + \frac{1}{\rho}\frac{\mathrm{d}R}{\mathrm{d}\rho} - \left(\frac{\delta_2}{a^2} + \frac{m^2}{\rho^2}\right)R = 0 \quad (a - \Delta \le \rho < a),$$
$$\frac{\mathrm{d}^2R}{\mathrm{d}\rho^2} + \frac{1}{\rho}\frac{\mathrm{d}R}{\mathrm{d}\rho} + \left(\frac{\delta_3}{a^2} - \frac{m^2}{\rho^2}\right)R = 0 \quad (\rho \ge a). \tag{11}$$

The height of the potential V_0 is very important for atomic motion inside the magnetic tube. We shall discuss the atomic motion for different V_0 in the following three cases.

3.1. In the case of $V_0 \gg \hbar^2/2Ma^2$

The height of the potential can be treated as infinity and the radial motion of the atom is discrete. The eigenwavefunction and eigenvalue of the energy can be determined by the following equations:

$$E_{m,n} = \frac{\hbar^2}{2M}\left(\frac{\lambda_{m,n}^2}{a^2} + \beta^2\right), \tag{12}$$

$$\Psi_{m,n}(\rho,\phi,z) = A\mathrm{J}_m\left(\lambda_{m,n}\frac{\rho}{a}\right)\mathrm{e}^{\mathrm{i}m\phi}\mathrm{e}^{\mathrm{i}\beta z}, \tag{13}$$

where $\lambda_{m,n}$ is the n-th root of Bessel function of m-order $\mathrm{J}_m(x)$=0 and A is a normalization factor. From the first root $\lambda_{0,1}$=2.40, the fundamental mode is determined, and we can estimate the corresponding temperature $T = 5.76\hbar^2/(2Ma^2k_\mathrm{B})$, in which a is the radius of the tube and M is the mass of the atom. For example, the temperature about 16 nK corresponds to the fundamental mode of ^{87}Rb atom in a magnetic tube with radius a=1μm.

3.2. In the case of $E - \hbar^2\beta^2/2M < V_0$

The atom will be trapped inside the tube in classical sense, however, it can tunnel out as a result of the finite width of the potential Δ, analogous to the "leaked out" mode in optical waveguide. In order to describe the transmission and the reflection of the atom wave, we use the following radial wavefunctions:

$$R(\rho) = \begin{cases} \mathrm{H}_\mathrm{m}^{(1)}\left(\sqrt{\delta_1}\frac{\rho}{a}\right) + A\mathrm{H}_\mathrm{m}^{(2)}\left(\sqrt{\delta_1}\frac{\rho}{a}\right) & (\rho < a - \Delta), \\ B\mathrm{I}_\mathrm{m}\left(\sqrt{\delta_2}\frac{\rho}{a}\right) + C\mathrm{K}_\mathrm{m}\left(\sqrt{\delta_2}\frac{\rho}{a}\right) & (a - \Delta \le \rho < a), \\ D\mathrm{H}_\mathrm{m}^{(1)}\left(\sqrt{\delta_3}\frac{\rho}{a}\right) & (\rho \ge a), \end{cases} \tag{14}$$

where $\mathrm{H}_\mathrm{m}^{(1)}$ and $\mathrm{H}_\mathrm{m}^{(2)}$ are the first and second kinds of Hankel function, and I_m and K_m are imaginary Bessel functions. And A, B, C and D can be determined by the continuity conditions of wavefunctions and their derivatives at the boundaries $\rho = a - \Delta$ and $\rho = a$, so that we obtain the following equations:

$$\begin{aligned}
&A\mathrm{H}_\mathrm{m}^{(2)}(\sqrt{\delta_1}(1-x)) - B\mathrm{I}_\mathrm{m}(\sqrt{\delta_2}(1-x)) - C\mathrm{K}_\mathrm{m}(\sqrt{\delta_2}(1-x)) = -\mathrm{H}_\mathrm{m}^{(1)}(\sqrt{\delta_1}(1-x)),\\
&A\mathrm{H}_\mathrm{m}^{(2)'}(\sqrt{\delta_1}(1-x))\sqrt{\delta_1/\delta_2} - B\mathrm{I}'_\mathrm{m}(\sqrt{\delta_2}(1-x)) - C\mathrm{K}'_\mathrm{m}(\sqrt{\delta_2}(1-x)) = -\mathrm{H}_\mathrm{m}^{(1)'}(\sqrt{\delta_1}(1-x))\sqrt{\delta_1/\delta_2},\\
&B\mathrm{I}_\mathrm{m}(\sqrt{\delta_2}) + C\mathrm{K}_\mathrm{m}(\sqrt{\delta_2}) - D\mathrm{H}_\mathrm{m}^{(1)}(\sqrt{\delta_3}) = 0,\\
&B\mathrm{I}'_\mathrm{m}(\sqrt{\delta_2}) + C\mathrm{K}'_\mathrm{m}(\sqrt{\delta_2}) - D\mathrm{H}_\mathrm{m}^{(1)'}(\sqrt{\delta_3})\sqrt{\delta_3/\delta_2} = 0,
\end{aligned} \tag{15}$$

where we use the same substitutions as those in deriving Eq.(11) and we define $x = \Delta/a$. From Eq.(15), A and D can be obtained by Cramer's rule in linear algebra.[10] Then the transmission coefficient T and the reflection coefficient R can be determined by the input probability flux density $j_{\rm i}$, reflection probability flux density $j_{\rm r}$ and transmission probability flux density $j_{\rm t}$, which are deduced by following equations:

$$j_{\rm i} = \frac{\hbar}{m}{\rm Im}\left(\mathrm{H}_{\rm m}^{(1)^*}\left(\sqrt{\delta_1}\frac{\rho}{a}\right)\frac{\partial \mathrm{H}_{\rm m}^{(1)}\left(\sqrt{\delta_1}\frac{\rho}{a}\right)}{\partial\rho}\right), \quad (16)$$

$$j_{\rm r} = \frac{\hbar}{m}{\rm Im}\left(A^*\mathrm{H}_{\rm m}^{(2)^*}\left(\sqrt{\delta_1}\frac{\rho}{a}\right)\frac{\partial A\mathrm{H}_{\rm m}^{(2)}\left(\sqrt{\delta_1}\frac{\rho}{a}\right)}{\partial\rho}\right), \quad (17)$$

$$j_{\rm t} = \frac{\hbar}{m}{\rm Im}\left(D^*\mathrm{H}_{\rm m}^{(1)^*}\left(\sqrt{\delta_3}\frac{\rho}{a}\right)\frac{\partial D\mathrm{H}_{\rm m}^{(1)}\left(\sqrt{\delta_3}\frac{\rho}{a}\right)}{\partial\rho}\right), \quad (18)$$

and $R = j_{\rm r}/j_{\rm i}$, $T = j_{\rm t}/j_{\rm i}$. Figure 4 illustrates the variation of the transmission and reflection coefficients of ^{87}Rb atom versus the transverse energy of the atom at different potential V_0. In the calculation, the parameters are Δ/a=0.1 and V_0=1, 10, 100 μK. It is clear from the Fig.4 that the tunnelling effect of the atomic wavepacket is more obvious at smaller V_0. We also calculate the transmission and reflection coefficients versus the width Δ of the potential V_0, and find that at narrower widths, the tunnelling effect is more obvious.

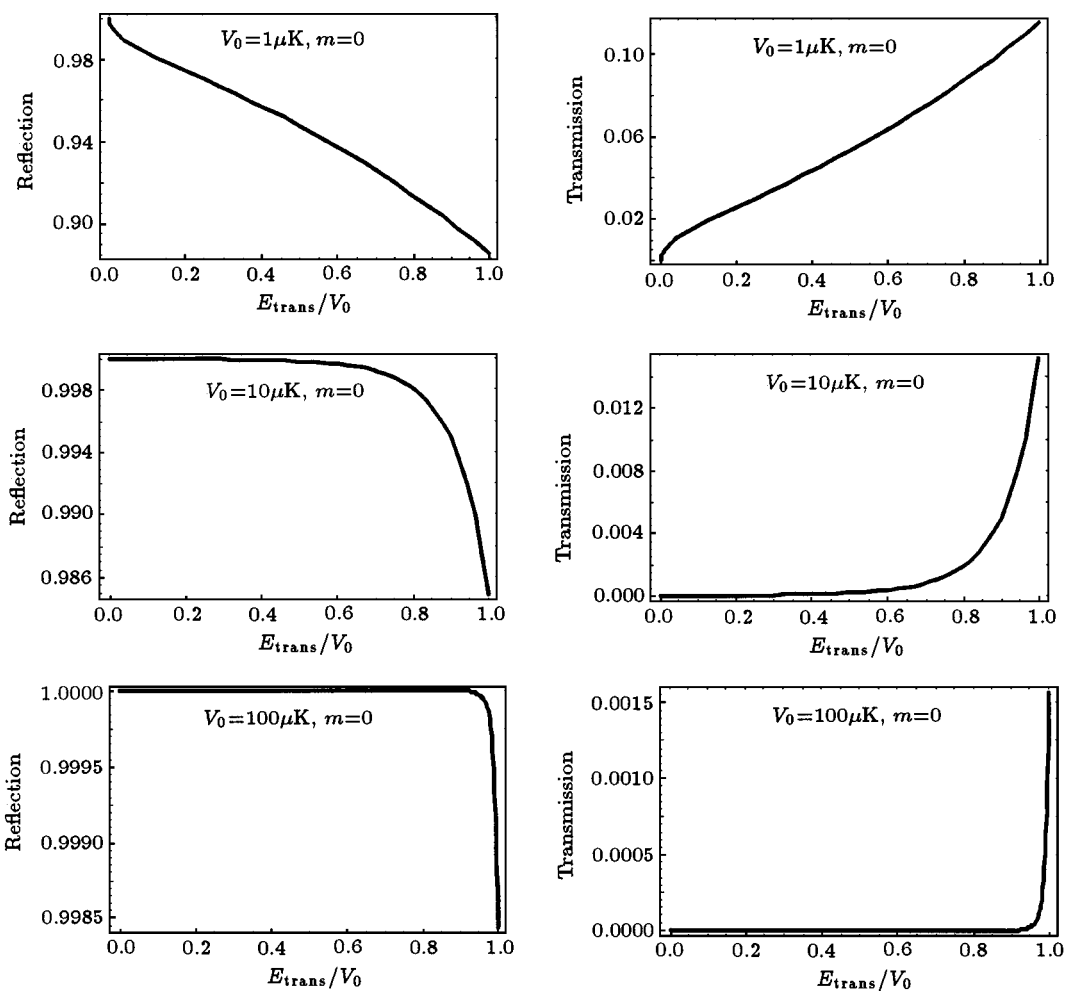


Fig.4. The curves of the transmission and reflection coefficients of ^{87}Rb atom versus the transverse energy of the atom at different potential V_0 in the case of $E - \hbar^2\beta^2/2M < V_0$.

3.3. In the case of $E - \hbar^2\beta^2/2M \geq V_0$

In this case, the atom cannot be trapped inside the waveguide. However, there exists reflection due to quantum effect. We can discuss the transmission and reflection by the same method as in Case 2. Figure 5 illustrates the calculation of transmission and reflection coefficients of ^{87}Rb atom versus the transverse energy of the atom. As shown in the Fig.5, there exists many peaks in the curves of transmission and reflection coefficients, which can be explained by quantum resonant effect.

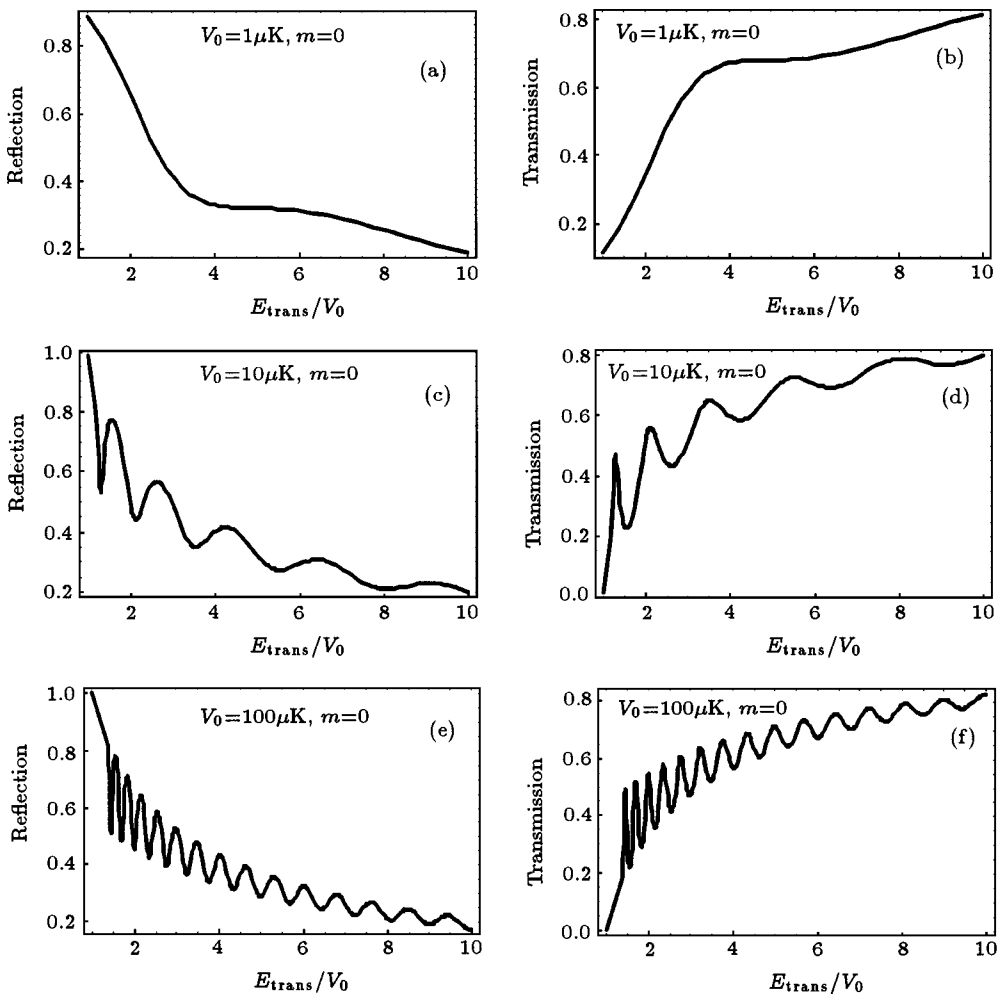


Fig.5. The transmission and reflection coefficients of ^{87}Rb atom versus the transverse energy of the atom in the case of $E - \hbar^2\beta^2/2M \geq V_0$.

4. The adiabatic motion condition of the atom inside the magnetic waveguide

In the Section 3, we discussed the quantized motion of the atoms inside the waveguide. The most important assumption is that the motion of the atom is adiabatic. However, the direction of the magnetic field inside the tube varies with the position, and the magnetic field only exists near the wall. The field is approximately zero near the centre of the tube, which is the reason that it is called "spin flip out" effect.[11] The atom will transit non-adiabatically because of these factors. In this section, we discuss how to solve the "zero magnetic field" problem and estimate the probability for non-adiabatic transitions among the different magnetic quantum states due to the directional variation of the magnetic field.

In order to overcome the "zero magnetic field" problem, a small bias magnetic field is needed. But in our magnetic tube, a fixed small bias magnetic field can only change the position of the "zero magnetic field". So we adopt the time orbit potential technique by using a rotational bias magnetic field (Fig.6). Due to the screening effect, directly applying a bias magnetic field is impossible. However, the rotational bias magnetic field can be created effectively by Raman technique.[12]

$$\boldsymbol{B}_{\rm bias}(x,y,t) = B_0\cos\Omega t\boldsymbol{e}_x + B_0\sin\Omega t\boldsymbol{e}_y, \qquad (19)$$

where B_0 is much smaller than the magnetic field at the wall of the tube and Ω is the angular velocity of the rotating magnetic field which satisfies the following condition:

$$\omega_{\rm a} \ll \Omega \ll \omega_{\rm L}. \qquad (20)$$

Here $\omega_{\rm L}$ is the Lamor frequency and $\omega_{\rm a}$ is the angular velocity of the atom. By this rotational bias magnetic field, the average magnetic field that the atom "feel" is

$$\begin{aligned} &B_{\rm av}(\rho,z,\phi)\\ =&\frac{\Omega}{2\pi}\int_0^{\frac{2\pi}{\Omega}} B(t)\mathrm{d}t\\ =&\frac{2}{\pi}\sqrt{B_0^2+B^2(\rho)-2B_0B(\rho)\sin kz}\\ &\times \mathrm{E}\left(-\frac{4B_0B(\rho)\sin kz}{B_0^2+B^2(\rho)-2B_0B(\rho)\sin kz}\right), \end{aligned} \qquad (21)$$

where $\mathrm{E}(m) = \int_0^{\frac{\pi}{2}} \sqrt{1-m\sin^2\varphi}\,\mathrm{d}\varphi$ is the elliptical function. It is not difficult to test that there is no zero point of $B_{\rm av}$.

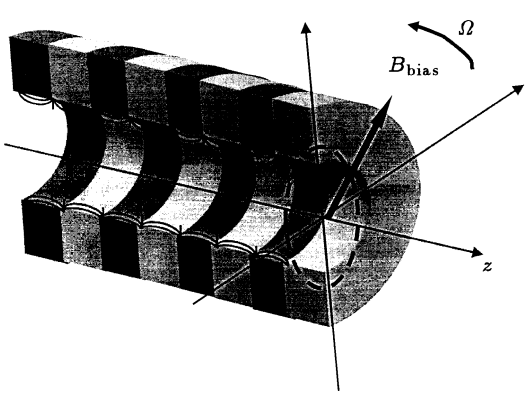


Fig.6. The time orbit potential technique by using a rotational bias magnetic field.

Now we discuss the non-adiabatic transition among the different magnetic quantum states due to the directional variation of the magnetic field that the atom "feel". In order to simplify the problem, here we only consider the alkali atom with total spin F=1 and assume the Lande factor $g_F > 0$ so that only M_F=1 state corresponding to the local magnetic field $|\uparrow\rangle$ can be trapped inside the magnetic field. The other two states, namely $|0\rangle$ and $|\downarrow\rangle$, corresponding to M_F=0, -1 respectively, cannot be trapped.

Assuming that at the initial time t_0, the atom is in state $|\uparrow\rangle$, that is

$$\psi(t_0) = |\uparrow\rangle, \qquad (22)$$

and the Schrödinger equation describes the evolution of the atomic wavefunction

$$|\psi(t)\rangle = \exp\left[-\frac{\mathrm{i}}{\hbar}\int_{t_0}^{t}\hat{H}(t)\mathrm{d}t\right]|\uparrow(t_0)\rangle. \qquad (23)$$

Then at time t, the probability of the atom still in state $|\uparrow(t)\rangle$ is

$$\begin{aligned} P =&|\langle\uparrow(t)|\psi(t)\rangle|^2\\ =&\left|\langle\uparrow(t)|\exp\left[-\frac{\mathrm{i}}{\hbar}\int_{t_0}^{t}\hat{H}(t)\mathrm{d}t\right]|\uparrow(t_0)\rangle\right|^2. \end{aligned} \qquad (24)$$

We note that $|\uparrow(t)\rangle$ is different from $|\uparrow(t_0)\rangle$ unless the magnetic field is uniform.

We discuss the non-adiabatic transition in the following two cases:

4.1. In the case of near the tube centre

In this case, the magnetic field can be described by Eq.(19). So the three states at time t can be written as

$$|\uparrow\rangle = \left(\frac{\mathrm{e}^{-\mathrm{i}\Omega t}}{2}\quad\frac{1}{\sqrt{2}}\quad\frac{\mathrm{e}^{\mathrm{i}\Omega t}}{2}\right)^{\mathrm{T}}, \qquad (25)$$

$$|0\rangle = \left(-\frac{\mathrm{e}^{-\mathrm{i}\Omega t}}{\sqrt{2}}\quad 0\quad\frac{\mathrm{e}^{\mathrm{i}\Omega t}}{\sqrt{2}}\right)^{\mathrm{T}}, \qquad (26)$$

$$|\downarrow\rangle = \left(\frac{\mathrm{e}^{-\mathrm{i}\Omega t}}{2}\quad-\frac{1}{\sqrt{2}}\quad\frac{\mathrm{e}^{\mathrm{i}\Omega t}}{2}\right)^{\mathrm{T}}. \qquad (27)$$

Since the distribution of the magnetic field near the centre is independent of its position, we can ignore the motion of the centre of mass of the atom in the Hamiltonian,

$$\hat{H}(t) = \frac{\hbar\omega_{\rm L}}{\sqrt{2}}\begin{pmatrix} 0 & \mathrm{e}^{-\mathrm{i}\Omega t} & 0\\ \mathrm{e}^{\mathrm{i}\Omega t} & 0 & \mathrm{e}^{-\mathrm{i}\Omega t}\\ 0 & \mathrm{e}^{\mathrm{i}\Omega t} & 0\end{pmatrix}. \qquad (28)$$

From Eqs.(27) and (28), we can calculate the population evolution in states $|\uparrow\rangle$, $|0\rangle$ and $|\downarrow\rangle$. Figure 7

illustrates the population evolution at different rotational frequencies of the bias magnetic field. When the rotational frequency $\Omega \ll \omega_{\mathrm{L}}$, there is no transition from $|\uparrow\rangle$ to $|0\rangle$ and $|\downarrow\rangle$, the atom will stay in its initial state $|\uparrow\rangle$. If the rotational frequency $\Omega \sim \omega_{\mathrm{L}}$, the atom will transit among the states $|\uparrow\rangle$, $|0\rangle$ and $|\downarrow\rangle$ periodically. So the condition $\Omega \ll \omega_{\mathrm{L}}$ is necessary for the atomic waveguide.

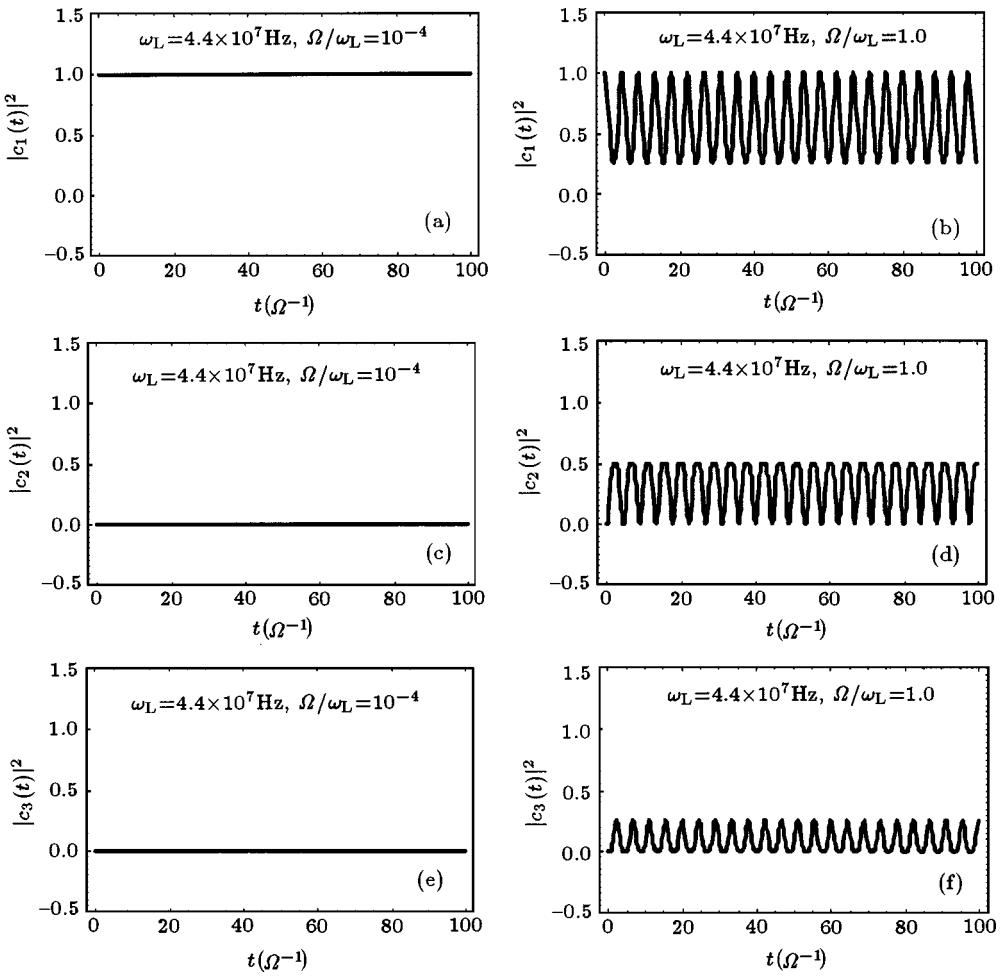


Fig. 7. The population evolution at different rotational frequencies of the bias magnetic field near the centre of the tube. (a), (c), (e) $\Omega \ll \omega_{\mathrm{L}}$. (b), (d), (f) $\Omega \sim \omega_{\mathrm{L}}$.

4.2. In the case of near the wall

We can ignore the bias field in this case. And the magnetic field takes the following form:

$$\begin{aligned}\boldsymbol{B} =& - B(a)\mathrm{e}^{-k(a-\rho)}\cos(kz)\boldsymbol{e}_z \\ & - B(a)\mathrm{e}^{-k(a-\rho)}\sin(kz)\boldsymbol{e}_\rho. \end{aligned} \tag{29}$$

And the three eigenstates related to the local magnetic field are

$$|\uparrow\rangle = \left(\mathrm{e}^{-\mathrm{i}\phi}\sin^2(kz/2) \quad -\frac{\sin kz}{\sqrt{2}} \quad \mathrm{e}^{\mathrm{i}\phi}\cos^2(kz/2)\right)^{\mathrm{T}}, \tag{30}$$

$$|0\rangle = \left(\frac{\sin kz}{\sqrt{2}}\mathrm{e}^{-\mathrm{i}\phi} \quad -\cos kz \quad -\frac{\sin kz}{\sqrt{2}}\mathrm{e}^{\mathrm{i}\phi}\right)^{\mathrm{T}}, \tag{31}$$

$$|\downarrow\rangle = \left(\mathrm{e}^{-\mathrm{i}\phi}\cos^2(kz/2) \quad \frac{1}{\sqrt{2}}\sin kz \quad \mathrm{e}^{\mathrm{i}\phi}\sin^2(kz/2)\right)^{\mathrm{T}}. \tag{32}$$

So near the wall the states $|\uparrow\rangle$, $|0\rangle$ and $|\downarrow\rangle$ depend on their positions. The Hamiltonian of the atom in the magnetic field can be expressed as

$$\begin{aligned}\hat{H} =& -\frac{\hbar^2}{2M}\nabla^2 + g_F\mu_{\mathrm{B}} \\ & \times (F_xB_\rho\cos\phi + F_yB_\rho\sin\phi + F_zB_z). \end{aligned} \tag{33}$$

In the (F^2, F_z) representation, the Hamiltonian has the following matrix form:

$$\hat{V} = \hbar\omega_{\rm L}(\rho)\begin{pmatrix} -\cos kz & -\frac{1}{\sqrt{2}}{\rm e}^{-{\rm i}\phi}\sin kz & 0 \\ -\frac{1}{\sqrt{2}}{\rm e}^{{\rm i}\phi}\sin kz & 0 & -\frac{1}{\sqrt{2}}{\rm e}^{-{\rm i}\phi}\sin kz \\ 0 & -\frac{1}{\sqrt{2}}{\rm e}^{{\rm i}\phi}\sin kz & \cos kz \end{pmatrix}, \tag{34}$$

$$\hat{T} = -\frac{\hbar^2}{2M}\nabla^2, \tag{35}$$

where

$$\omega_{\rm L}(\rho) = \frac{g_F\mu_{\rm B}B(a){\rm e}^{-k(a-\rho)}}{\hbar} \tag{36}$$

is the Lamor frequency.

Now we will change the representation to $|\uparrow\rangle$, $|0\rangle$ and $|\downarrow\rangle$, the transformation matrix is

$$U = \begin{pmatrix} {\rm e}^{-{\rm i}\phi}\sin^2(kz/2) & \frac{\sin kz}{\sqrt{2}}{\rm e}^{-{\rm i}\phi} & {\rm e}^{-{\rm i}\phi}\cos^2(kz/2) \\ -\frac{\sin kz}{\sqrt{2}} & -\cos kz & \frac{1}{\sqrt{2}}\sin kz \\ {\rm e}^{{\rm i}\phi}\cos^2(kz/2) & -\frac{\sin kz}{\sqrt{2}}{\rm e}^{{\rm i}\phi} & {\rm e}^{{\rm i}\phi}\sin^2(kz/2) \end{pmatrix} \tag{37}$$

and the form of Hamiltonian in $|\uparrow\rangle$, $|0\rangle$ and $|\downarrow\rangle$ representation is

$$\hat{V}' = \hbar\omega_{\rm L}(\rho)\begin{pmatrix} 1 & 0 & 0 \\ 0 & 0 & 0 \\ 0 & 0 & -1 \end{pmatrix}, \tag{38}$$

$$\hat{T}' = U^{\dagger}\hat{T}U. \tag{39}$$

The kinetic energy function can be expanded as[13]

$$\hat{T}' = \hat{T} + \frac{1}{2M}(\hat{p}\cdot\hat{A} + \hat{A}\cdot\hat{p}) + \frac{1}{2M}\hat{A}\cdot\hat{A}, \tag{40}$$

where $\hat{p}$ is the momentum operator $-{\rm i}\hbar\nabla$ and $\hat{A} = -{\rm i}\hbar U^{+}(\nabla U)$.

So in $|\uparrow\rangle$, $|0\rangle$ and $|\downarrow\rangle$ representation the Hamiltonian describing the atomic motion near the wall can be expressed as

$$\hat{H}' = \begin{pmatrix} -\frac{\hbar}{2M}\nabla^2 + \hbar\omega_{\rm L}(\rho) & 0 & 0 \\ 0 & -\frac{\hbar^2}{2M}\nabla^2 & 0 \\ 0 & 0 & -\frac{\hbar^2}{2M}\nabla^2 - \hbar\omega_{\rm L}(\rho) \end{pmatrix} + \frac{1}{2M}(\hat{p}\cdot\hat{A} + \hat{A}\cdot\hat{p}) + \frac{1}{2M}\hat{A}\cdot\hat{A}. \tag{41}$$

The first term is the Hamiltonian for adiabatic motion, and the non-adiabatic transitions among $|\uparrow\rangle$, $|0\rangle$ and $|\downarrow\rangle$ are the results of the last two terms, which we named non-adiabatic Hamiltonian. The non-adiabatic Hamiltonian is related to the momentum of the atom. This is because the momentum is small for the cold atom. We estimate the non-adiabatic transition by method of perturbative analysis, and the probabilities for the non-adiabatic transition can be estimated by the following equations:

$$P_{\uparrow\to 0}(t) = \frac{1}{\hbar^2}|\langle 0,\varphi_0(r)|H_1'|\uparrow,\varphi_{\uparrow}(r)\rangle|^2\frac{\sin^2(\omega_{\rm L}t/2)}{(\omega_{\rm L}/2)^2}, \tag{42}$$

$$P_{\uparrow\to\downarrow}(t) = \frac{1}{\hbar^2}|\langle\downarrow,\varphi_{\downarrow}(r)|H_1'|\uparrow,\varphi_{\uparrow}(r)\rangle|^2\frac{\sin^2(\omega_{\rm L}t)}{\omega_{\rm L}^2}, \tag{43}$$

where $\varphi_{\uparrow}(r)$, $\varphi_0(r)$ and $\varphi_{\downarrow}(r)$ are the wavefunctions describing the atomic motion, and we use the average value of ω_{L} near the wall for estimation. For example, if the wavefunction describing the atomic motion is $\varphi \sim \exp(\mathrm{i}m\nu_z z/\hbar)$, we can obtain the probabilities in the following form:

$$P_{\uparrow\to 0}(t) = \frac{1}{\hbar^2}\left|\mathrm{i}\frac{\hbar k\nu_z}{\sqrt{2}} + \frac{17\hbar^2k^2}{64\sqrt{2}M}\sin 2kz\right|^2 \frac{\sin^2(\omega_{\mathrm{L}}t/2)}{(\omega_{\mathrm{L}}/2)^2}, \tag{44}$$

$$P_{\uparrow\to\downarrow}(t) = \frac{1}{\hbar^2}\left|\frac{\hbar^2k^2}{64M}(11 + 8\cos kz - 2\cos 2kz - \cos 4kz)\right|^2 \frac{\sin^2(\omega_{\mathrm{L}}t)}{\omega_{\mathrm{L}}^2}. \tag{45}$$

Finally, we find the condition for the adiabatic motion of the atom to be

$$k\nu_z \ll \omega_{\mathrm{L}}, \tag{46}$$

$$\frac{\hbar k^2}{M} \ll \omega_{\mathrm{L}}. \tag{47}$$

This means that in order to prevent the non-adiabatic transition, the motion of the atom should be slow and the period of the magnetization cannot be too small.

5. Discussion and Conclusion

In this paper we have discussed the quantized motion of the cold atom inside the magnetic atom waveguide we proposed before. We discussed in detail the motion of the atomic wavepacket, including the mode, quantum tunnelling effect, and probability for the non-adiabatic transition. These discussions are essential for the estimation of the atomic transport efficiency and will shed light on the design of the atomic waveguide devices.

Acknowledgment

The author Li Dai-Jun would like to thank Professor Zhang Wei-Ping for many useful discussions on the paper.

References

[1] Pritchard D E *et al* 2001 *Ann. Phys., Lpz.* **10** 35
[2] Leveque G *et al* 2002 *Phys. Rev.* A **65** 53615
[3] Carusotto I and La Rocca G C 2000 *Phys. Rev. Lett.* **84** 399
[4] Leggett A J 2001 *Rev. Mod. Phys.* **73** 307
[5] Li D J, Huang H, Lu X H and Li S Q 1999 *Opt. Commun.* **160** 72
[6] Liu X J, Li D J, Wang D Z, Huang H and Li S Q 2001 *Chin. Phys. Lett.* **18** 724
[7] Li D J, Hu Z F and Li S Q 2003 *Chin. Phys.* **12** 738
[8] Minogin V G, Richmond J A and Opat G I 1998 *Phys. Rev.* A **58** 3138
[9] Hinds E A, Boshier M G and Hughes I G 1998 *Phys. Rev. Lett.* **80** 645
[10] Gradshteyn I S and Ryzhik I M 1980 *Table of Integrals, Series and Products* (New York: Academic) p1110
[11] Petrich W *et al* 1995 *Phys. Rev. Lett.* **74** 3352
[12] Marzlin K P, Zhang W and Wright E M 1997 *Phys. Rev. Lett.* **79** 4728
[13] Sukumar C V and Brink D M 1997 *Phys. Rev.* A **56** 2451